

# UC Riverside

## UC Riverside Electronic Theses and Dissertations

### Title

Cell and Particle Sorting Using Lateral Flow in Woven Meshes

### Permalink

<https://escholarship.org/uc/item/59v9m65t>

### Author

Patel, Tejas

### Publication Date

2014

Peer reviewed|Thesis/dissertation

UNIVERSITY OF CALIFORNIA  
RIVERSIDE

Cell and Particle Sorting Using Lateral Flow in Woven Meshes

A Thesis submitted in partial satisfaction  
of the requirements for the degree of

Master of Science

in

Bioengineering

by

Tejas Patel

December 2014

Thesis Committee:

Dr. William H. Grover, Chairperson

Dr. B. Hyle Park

Dr. Masaru P. Rao

Copyright by  
Tejas Patel  
2014

The Thesis of Tejas Patel is approved:

---

---

---

Committee Chairperson

University of California, Riverside

## TABLE OF CONTENTS

<b>LIST OF FIGURES</b> .....	v
<b>1 INTRODUCTION</b> .....	1
1.1 MOTIVATION .....	1
<b>2 BACKGROUND</b> .....	2
2.1 CURRENT METHODS OF MICROFLUIDIC CELL SORTING .....	2
2.2 PASSIVE SEPARATION .....	3
2.2.1 DETERMINISTIC LATERAL DISPLACEMENT DEVICE .....	4
2.2.2 DETERMINISTIC CELL ROLLING DEVICE .....	7
2.3 DISADVANTAGES.....	8
2.3.1 FABRICATION TIME AND COMPLEXITY .....	9
2.3.2 EQUIPMENT COST .....	9
<b>3 SPECIFIC AIMS</b> .....	10
3.1 MICRO FEATURED MESH .....	11
3.2 SPECIFIC AIMS I.....	11
3.2.1 RIGID FLOW-THROUGH DEVICE.....	12
3.2.2 FLEXIBLE FLOW THROUGH DEVICE.....	14
3.3 SPECIFIC AIMS II .....	16
3.3.1 CHANNEL DESIGN .....	17
3.3.2 FABRICATION .....	18
3.3.3 ASSEMBLY.....	19
3.4 SPECIFIC AIM III .....	20
3.4.1 EXPERIMENTAL DESIGN .....	20
3.4.2 FLOW-THROUGH RESULTS.....	21
3.4.3 FLOW OVER RESULTS.....	27
<b>4 CONCLUSION</b> .....	33
4.1 FLOW-THROUGH DEVICE.....	33
4.2 FLOW OVER DEVICE .....	33
4.3 FUTURE WORKS.....	34
<b>5 REFERENCES</b> .....	35

## LIST OF FIGURES

<b>FIGURE 1:</b> Schematic of Dielectrophoresis .....	<b>3</b>
<b>FIGURE 2:</b> Schematic of DLD Device .....	<b>3</b>
<b>FIGURE 3:</b> Post Array with Flow Laminas .....	<b>5</b>
<b>FIGURE 4:</b> Post Array with Parameters .....	<b>6</b>
<b>FIGURE 5:</b> Schematic of Roll Over Device .....	<b>7</b>
<b>FIGURE 6:</b> Schematic of Deep Reactive Ion Etching .....	<b>9</b>
<b>FIGURE 7:</b> Image of Micro-Woven Mesh .....	<b>11</b>
<b>FIGURE 8:</b> Schematic of Rigid Flow-Through Device Assembly .....	<b>12</b>
<b>FIGURE 9:</b> Image of Assembled Rigid Device .....	<b>13</b>
<b>FIGURE 10:</b> Schematic of Flexible Flow-Through Device Assembly .....	<b>14</b>
<b>FIGURE 11:</b> Image of Assembled Flexible Device .....	<b>15</b>
<b>FIGURE 12:</b> Image of Assembled Roll Over Device .....	<b>16</b>
<b>FIGURE 13:</b> Computational Model of Device Flow Focusing .....	<b>17</b>
<b>FIGURE 14:</b> Schematic of Roll Over Device Assembly .....	<b>19</b>
<b>FIGURE 15:</b> Schematic of Experimental Setup .....	<b>20</b>
<b>FIGURE 16:</b> Fluorescent Image of Head Pressure Driven Flow of 5 Micron Beads Through the Rigid 78 Micron Mesh .....	<b>22</b>
<b>FIGURE 17:</b> Fluorescent Image of Head Pressure Driven Flow of 5 Micron Beads Through the Rigid 78 Micron Mesh .....	<b>23</b>
<b>FIGURE 18:</b> Fluorescent Image of Head Pressure Driven Flow of 5 Micron Beads Through the Rigid 78 Micron Mesh .....	<b>24</b>

**FIGURE 19:** Fluorescent Image of Vacuum Driven Flow of 5 Micron Beads Through the Rigid 78 Micron Mesh .....**25**

**FIGURE 20:** Fluorescent Image of Head Pressure Driven Flow of 5 Micron Beads in a Roll Over Device with a 27 Micron Mesh .....**28**

**FIGURE 21:** Fluorescent Image of Head Pressure Driven Flow of 5 Micron Beads in a Roll Over Device with a 27 Micron Mesh .....**29**

**FIGURE 22:** Fluorescent Image of Vacuum Driven Flow of 5 Micron Beads in a Roll Over Device with a 27 Micron Mesh .....**30**

**FIGURE 23:** Fluorescent Image of Vacuum Driven Flow of 5 Micron Beads in a Roll Over Device with a 27 Micron Mesh .....**32**

**FIGURE 24:** Fluorescent Image of Vacuum Driven Flow of 5 Micron Beads in a Roll Over Device with a 27 Micron Mesh .....**33**

## **1. INTRODUCTION**

Cell separation is a major sample processing step for many biological and medical assays.<sup>[1]</sup> Currently in a clinical setting, cell separation is usually achieved through centrifugation. Although centrifugation has a long history of use in clinical settings, it does have its drawbacks. The first drawback is the equipment required to sort cells using a centrifuge: Larger samples and higher G-forces can require large centrifuges. Centrifuges require specific consumables in the form of centrifuge tubes. Centrifugation is an example of a process with low “walkaway time”: personnel are required to wait by the process to start and finish it. This requires trained personnel, which increases assay cost and raises the possibility of human error. Trained personnel can be avoided by automating using robotics, but in practice the additional expense of robotic sample handlers is prohibitive in most clinical settings. Some procedures require resuspending cells/particles/etc. in different fluids multiple times. This can result in a lot of repetition between spin/rinse/resuspend steps. Finally, some fluids used to resuspend cells can also be toxic if left in cell for too long, and chemical exposures shorter than a few minutes are difficult to attain in centrifuges.

### **1.1 MOTIVATION**

Clinical analysis of blood often requires separation of plasma from its cellular components. Therefore, the most fundamental application for a cell sorting device is



separating cells from their surrounding fluid. A continuous flow through device would make separating the cellular components from the plasma a fast and efficient process.

For more specific cell sorting such as isolating circulating tumor cells (CTCs), centrifugation is not the best option. CTCs are extremely rare, estimated to be 1 tumor cell to 1 billion healthy cells in circulation, making them very difficult to isolate. This greatly increases the need for a precise and high throughput device to isolate circulating tumor cells.

A great alternative to centrifugation could be the utilization of microfluidics for cell sorting. Microfluidics allows us to work at the scale of the cells making the process faster and more efficient. <sup>[4]</sup>

## **2. BACKGROUND**

### **2.1 CURRENT METHODS OF MICROFLUIDIC CELL SORTING**

The current methods of microfluidic cell sorting can be broken down into active and passive sorting. <sup>[1,2]</sup> Active separation requires cells to be sorted based on external forces. An example of active separation is shown in Figure 1. This device uses nonuniform AC electric fields on cells and particles to manipulate them due to their ability to be polarized.

Passive separation relies on internal forces generated by arrays of cell-sized features which move particles or cells to different locations based on their sizes, densities, or adhesion properties. [3] This work focuses on passive separation techniques, which are examined more closely in the next section.

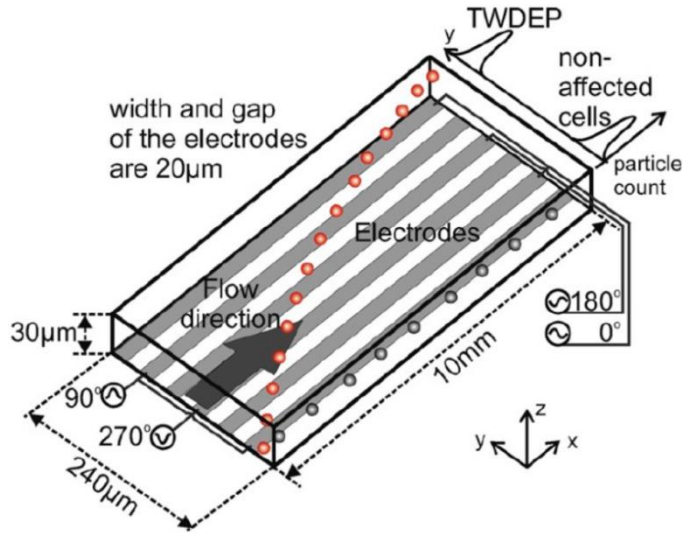


Figure 1: Dielectrophoresis device that induces a dipole to sort cells

## 2.2 PASSIVE SEPARATION

Passive sorting relies on unique geometries within the device that sort based on parameters such as size, density, deformability, and adhesive properties. Deterministic lateral displacement (DLD) devices and deterministic cell rolling devices are

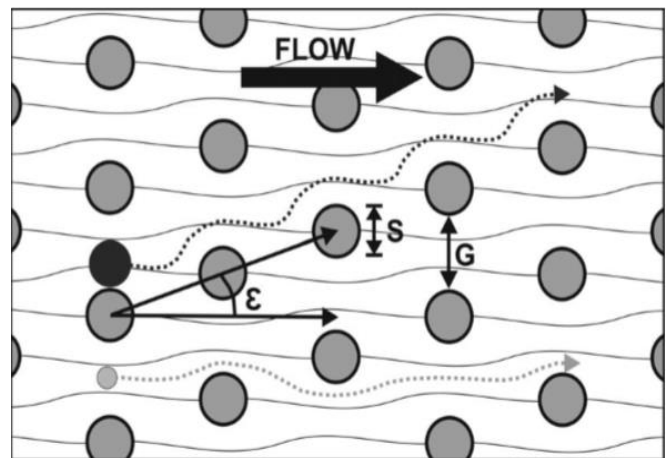


Figure 2: DLD device with an array of posts to displace large particles [4]

two passive techniques that will be discussed in further detail. These techniques take advantage of fluid flow in the micro scale by exhibiting laminar flow due to very low

Reynolds number ( $Re < 1$ ) at which viscous forces (not convective forces) are dominant. As a result, when two flow laminas meet in a DLD chip, they are said to flow in parallel without mixing as they flow through the device.<sup>[3,5]</sup>

### **2.2.1 DETERMINISTIC LATERAL DISPLACEMENT (DLD) DEVICES**

The first method of passive cell separation examined here is the deterministic lateral displacement (DLD) device. In such devices, numerous cell-sized features are arrayed with a consistent shift between rows (see Figure 3). The shifting of the array will create multiple but consistent flow lamina through the device. The presence of multiple flow laminas that consistently flow throughout the device can be exploited to sort particles. A particle flowing through a lamina will continue to flow through that same flow lamina for the duration of the device if its center of mass remains within the flow lamina.<sup>[7,8]</sup>

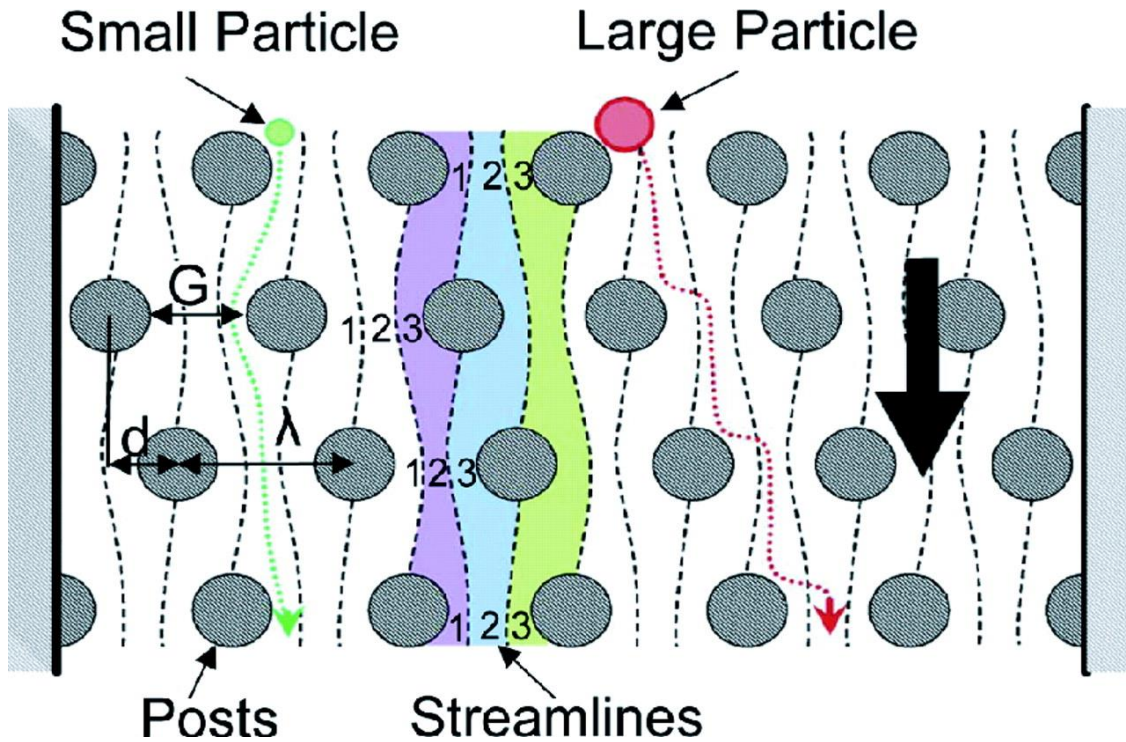


Figure 3: DLD device with post array showing different flow lamina and flow of two different sized particles through the array of post.<sup>[6]</sup>

Figure 3 illustrates how cells and particles are sorted in DLD devices. A small particle, depicted in green, will stay in its lamina until it approaches an obstacle. If the particle is small enough that its center of mass will remain in its original lamina, it will flow around the obstacle but still remain in the original lamina. The particle will therefore follow its lamina, zigzagging its way through the device with no net lateral movement. When this occurs the particle is said to be in zigzag mode.

When the larger particle depicted in red in Figure 3 approaches its first obstacle, the particle's relatively large size causes its center of mass to enter the neighboring lamina. When the particle approaches the next obstacle it will again be displaced into the next

lamina. This phenomenon continues throughout the device forcing the larger particle to be displaced at the angle of the array.

The factors that determine what particles can be sorted are: diameter of obstacle, distances between the obstacle, and the angle at which they are shifted.

$$N = \frac{\lambda}{\Delta\lambda} \quad (1)$$

$$\varepsilon = \frac{\Delta\lambda}{\lambda} = \frac{1}{N} = \tan\theta \quad (2)$$

$$D_C = 1.4G\varepsilon^{0.48} \quad (3)$$

The ratio of the distance between the center of neighboring post, represented by  $\lambda$ , and the distance of the center to center shift represented by  $\Delta\lambda$  with gives the number of laminae flowing between each post as shown

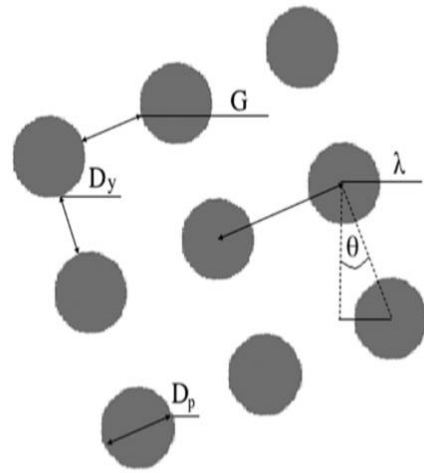


**Figure 4: Post array with key measurement needed for flow lamina and critical diameter calculations<sup>[9]</sup>**

by Equation (1). The row shift fraction can be calculated by taking the inverse of the flow laminae or by taking the tangent of the shift angle  $\theta$  as seen in Equation (2). The row shift fraction is then used to get the critical diameter using Equation (3) which defines the critical diameter at which a particle will exhibit displacement mode.<sup>[9]</sup>

## 2.2.2 DETERMINISTIC CELL ROLLING DEVICE

Like DLD devices, cell rolling devices rely on unique designs which cause particle to sort based on their size or binding affinity. Unlike DLD devices, roll-over devices combine flow over and flow through to sort particles. Roll-over devices are made with slanted ridges along the bottom of the channel that lead to a gutter to which the target particles are moved.<sup>[11]</sup> Above the ridges is space for other particles to flow. This creates two directions of flow: below the slanted ridges the flow tends towards the gutter; and above the ridges the flow follows a helical pattern in which non-target particles that venture to the gutter side will be cycled back to the focusing side.

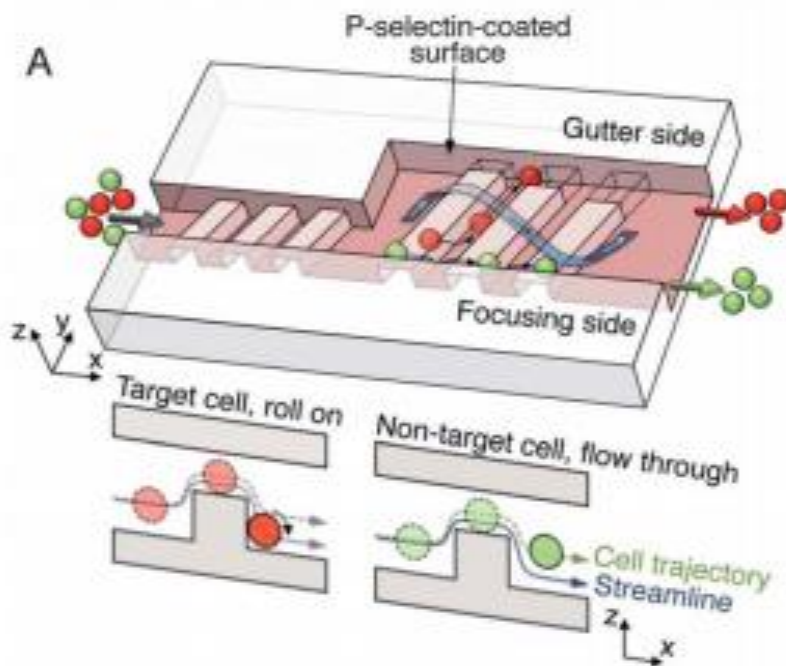


Figure 5: Roll over device utilizing both hydrophoresis and cell rolling due to adhesion to separate particles<sup>[11]</sup>

Figure 5 illustrates how a roll-over separation system works. Two types of particles are being introduced into the device represented by the red and green spheres. Roll-over devices use a combination of hydrophoresis and cell rolling to sort particles. <sup>[11]</sup> Particles encounter the ridges and follow the flow stream lines which prevent the particles from settling into the ridge completely depicted figure 5 bottom right. This effect is known as hydrophoresis. The target particles (red) behave differently when they encounter the ridges because the ridges are coated to have molecular interactions with the target particle. When a red particle comes in contact with the ridges, it begins to roll along the ridge and then into the ridge due to these molecular interactions, as shown in Figure 5. These target particles then roll along the slanted ridge into the gutter. The particles can then be collected downstream with the target particles on one side and other particles on the opposite side.

### **2.3 DISADVANTAGES OF CURRENT DEVICES**

Deterministic lateral displacement and deterministic cell rolling devices have been around for 10 years. What started as circular pillar has evolved to various geometric shapes and designs to optimize cell or particle separation. However, these technologies are still not widely applied for clinical uses. An explanation for this could be that the time and complexity of fabricating these devices outweighs the benefits of the devices. Along with the complexity, the equipment required to fabricate these devices can be very expensive.

### 2.3.1 FABRICATION TIME AND COMPLEXITY

The fabrication process required to make a DLD device usually requires deep reactive ion etching (DRIE). Deep reactive ion etching can be a complex and time consuming process. In order to achieve a high aspect ratio feature a passivation step is required after each etching step to protect the sides of the pillar. This cycle of etching and passivation is continued until the desired etch depth is obtained. The time required for this process can become quite long.

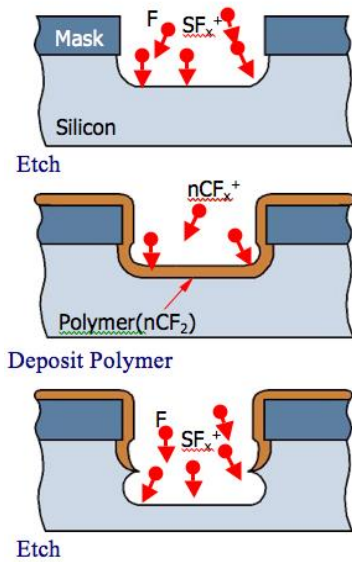


Figure 6: schematic of deep reactive ion etching (DRIE)

Fabrication of deterministic cell rolling devices can be even more complicated. Due to the multiple channel heights, the passivation steps can become more frequent and complicated. Multiple photomasks and multiple photolithography steps are needed to create the different channel heights in these devices.

### 2.3.2 EQUIPMENT COSTS

The process of making DLD and roll-over devices requires a number of expensive and specialized instruments. DLD and roll-over devices are usually made using silicon



wafers. A spin coater is used to deposit the photoresist. Once the wafer and its protective layer are in place the wafer is ready for the photolithography step. A contact aligner is used to align and expose the photoresist-coating using UV light. After developing the photoresist, the deep reactive ion etching can begin. After the fabrication steps are complete, the device is bonded to seal the device using an anodic bonder. Looking at the complete list of equipment (silicon wafer, spin coater, oven, contact aligner, deep reactive ion etcher, and anodic bonder), it is apparent that there could be major cost efficiency issues.

When one considers the time it takes to fabricate these devices and the complexity of fabrication behind them, as well as with the cost of materials and equipment required to fabricate these devices, it becomes very apparent why these devices are not used at the point of care in a disposable manner.

### **3. SPECIFIC AIMS**

Our aim is to develop a mass producible microfluidic device for sorting particles and cells based on their sizes, for point of care use, using micro woven meshes, and to conduct preliminary experiments to determine the effectiveness of these devices.

### **3.1 MICRO FEATURED MESH**

Deterministic lateral displacement (DLD) devices utilize highly uniform geometries to separate particles based on their size. We believe the principles that make DLDs so effective at sorting particles based on their size can be achieved using lateral flow through

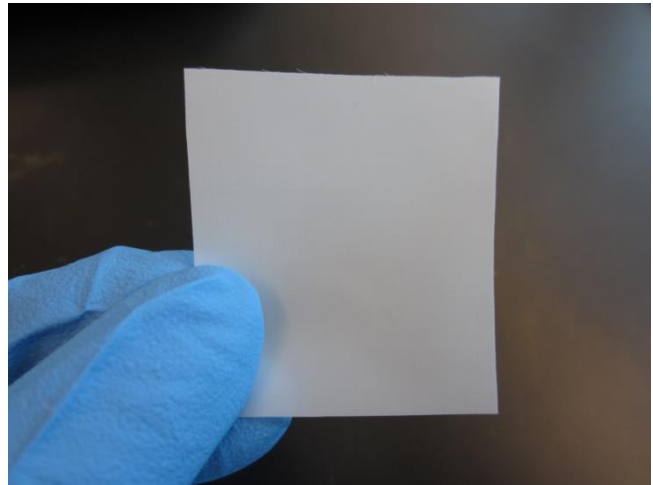


**Figure 7: Image of micro woven mesh**

commercially-available micro woven meshes. The precise arrangement of obstacles that result in predictable particle trajectories can be readily obtained using a woven mesh. We hypothesize that the uniform pattern of a woven mesh can create an arrangement of obstacles that allow for particles of various sizes to behave differently based on their size.

### **3.2 SPECIFIC AIM I**

The first specific aim was to fabricate a device that can achieve bump array like particle sorting using commercially available meshes. For a woven mesh to exhibit bump-array-like displacement of particles, the particles have to flow in the plane of the mesh. The “over-under” nature of a woven mesh give particles a 3-dimensional structure with which to interact. To achieve a flow-through device, the mesh must be covered or sealed on each side. Then the areas of the mesh where the mesh fibers go over and under each

other can be treated as a pillar. Because the mesh is contained on either side, in areas where the threads are over and under, particles are forced to flow around the mesh. If three major parameters are optimized, particles should behave the way they do in a DLD device. The three principles are thread size, pore size, and angle of mesh. The thread size will dictate the size of the pillar like obstacle that forms when there is an over under design of mesh. By controlling the pore size, we can control the spacing of the obstacles. Lastly, angling the mesh will result in a row shift. The row shift will cause multiple flow laminas, and coupled with obstacle size and spacing, a critical diameter can be calculated. The critical size tells what size a particle has to be in order to exhibit displacement.

### **3.2.1 RIGID FLOW THROUGH DEVICE**

In order to achieve lateral flow through a mesh we developed a rigid device where a piece of mesh is placed between two

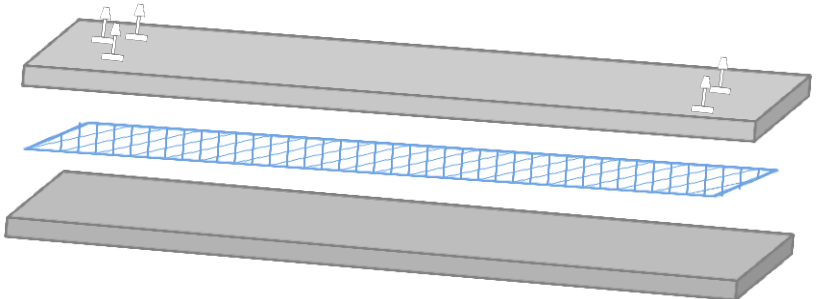


**Figure 8: Schematic of rigid device assembly. Mesh in blue placed between glass slide.**

glass microscope slides. The mesh is cut to the exact size of the glass slides. One piece of glass has adaptors attached to it from where fluid can enter and leave the device. The adaptors are placed strategically to focus the flow allowing particles to enter the device as close to the center as possible. This gives the particles the ability to be displaced in either direction. Current devices will send in particles through a channel just large enough to

allow a single cell to enter at a time. This is done to prevent particle to particle interaction as they are flowing through the device. Focusing the flow pinches the flow allowing fewer particles to enter at once. The other side of the device is a plain glass slide. The mesh being placed between two slides allows us to use meshes of any size. The device is then sealed using a quick set 5 minute epoxy. The epoxy is spread carefully around the edges of the glass slides to seal the device. After multiple uses the epoxy may wear out under high pressures and the device will leak. Repairing leaks can be as simple as applying more epoxy to a certain area or replacing the epoxy.

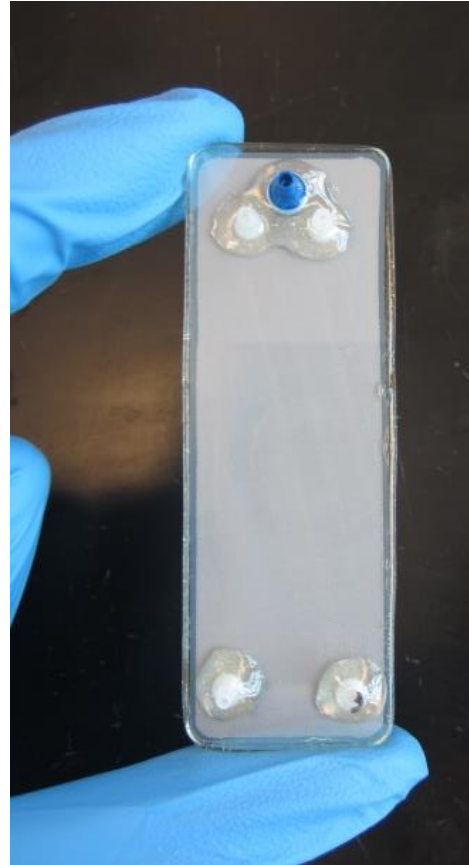


**Figure 9: Image of assembled rigid flow through device**

Fabricating a device of this nature is very quick and very inexpensive compared to classic bump array devices. No microfabrication is needed for the assembly of this device because the mesh contains the micron level features that allow for cell sorting. The materials needed to assemble this device are extremely cheap. One square inch of mesh costs 17 cents while each glass slide costs 14 cents. Compared to the cost of current

microfabricated bump array devices this can be a great alternative for disposable point of care use.

In microfluidic devices, air bubbles that become trapped inside the device can become a major problem. In an instance where air gets into the device, the flow is greatly disrupted. To limit the amount of air trapped in device, the fluid was degassed before introducing it into the device.

### **3.2.2 FLEXIBLE FLOW THROUGH DEVICE**

Much like the rigid flow-through device, the flexible device we developed also needs to contain the mesh from top and bottom if it is to act as a bump array

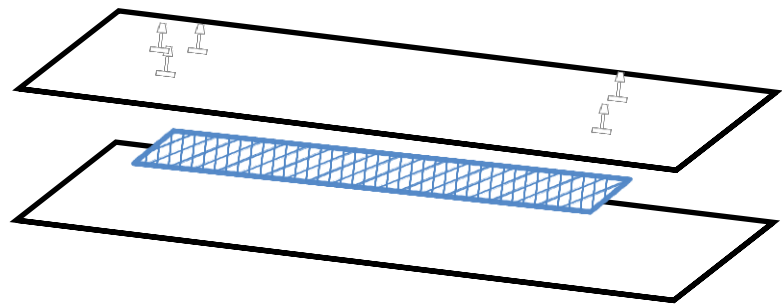


**Figure 10: Schematic of rigid device assembly. Mesh in blue placed between two sheets of laminate**

device. This device is fabricated by placing a piece of mesh between two sheets of plastic laminate. Unlike the rigid device, the mesh needs to be cut slightly smaller than the laminate sheet from all sides. This is done to allow the laminate to form a strong bond and prevent leaks. Once the mesh is placed between the laminate sheets, it is sent through a thermal laminator. One pass through the laminator is enough to seal the mesh inside the

laminated. The laminator seals the laminate by applying pressure and heat to melt the plastic sheets and form a strong bond.

One side of the laminate has holes punched to allow flow in and out of the device. Much like the rigid device, the flexible device also has adaptors placed strategically to focus the flow. In contrast to the rigid device, the flexible device cannot be used for all mesh sizes. Meshes with a pore size larger than 27 micron will be filled by the melting plastic as the device goes through the laminator.

The flexible device is extremely time and cost efficient. The laminator makes assembling the device even easier than the rigid device. The epoxy sealing methods require time to cure whereas the laminate is ready for use seconds after it comes out of the laminator. Also, the bond between the

laminated materials is much stronger than that of the epoxy for the rigid device. As mentioned before, the epoxy can weaken and leak under high pressures whereas the laminated seal holds up very well against high pressures. Fluids should be degassed before

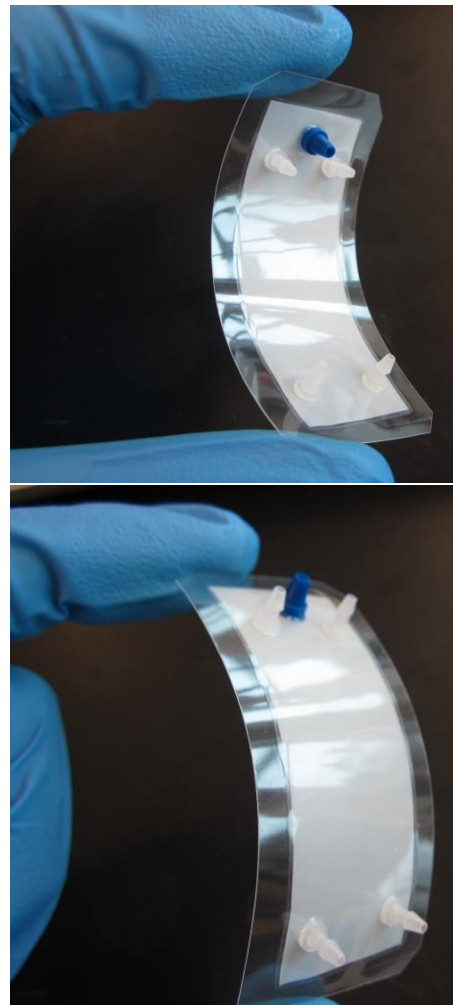


**Figure 11: Image of assembled flexible devices**

using in the device to prevent formation of air bubbles under high pressures. Another quality that both the rigid and flexible devices share is their cost effectiveness. A square inch of mesh costs 17 cents. A sheet of laminate cost 30 cents. Each sheet can produce ten or more devices, or 3 cents for laminate per device.

Both of these devices make a compelling alternative to current micro fabricated devices for exposable point of care use.

### **3.3 SPECIFIC AIM II**

In this aim, we set out to fabricate a roll-over sorting device using a mesh. Unlike the flow-through device, in order to achieve roll over sorting effects, particles can only interact with one side of the mesh. To accomplish this, we etched a channel into a glass wafer.



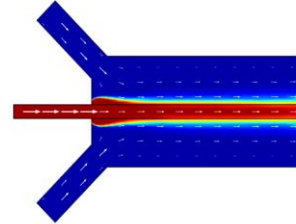
**Figure 12: Image of assembles flow over device**

Inside the wafer we placed the mesh and sealed it with a sheet of laminate. The laminate allowed for the channel to be sealed and also bonded to one side of the mesh. This meant that particles flowing through the device were not able to travel through the mesh; instead, the particles were forced to roll along the top of the mesh.

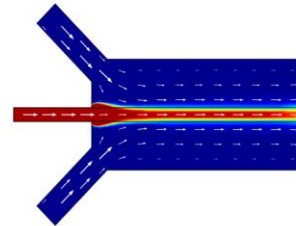
### 3.3.1 CHANNEL DESIGN

To allow for cells to settle and roll along the mesh, a channel was etched into glass wafers. The channel was designed to allow particles to settle by creating a 70  $\mu\text{m}$  channel. The channel was designed in such a way that the particles entering the device will enter in a focused manner in the middle of the device. This allows us to determine which direction the mesh will displace the particles. Also, by focusing the flow, particles are introduced in a linear manner decreasing the chances of particles interacting with each other causing false displacement. This was achieved using flow focusing to pinch the flow. This can be done by adjusting the flow rate between different inlets or by adjusting the channel sizes to increase resistance in a particular inlet causing differences in flow rates. Conventionally, flow focusing is achieved by adjusting the flow rate. Figure

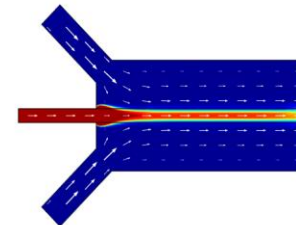
shearVel(2)=4.166667e-10 Time=0 s Surface: Concentration (mol/m<sup>3</sup>) Arrow Surface: Velocity field



shearVel(3)=8.333333e-10 Time=0 s Surface: Concentration (mol/m<sup>3</sup>) Arrow Surface: Velocity field



shearVel(4)=1.25e-9 Time=0 s Surface: Concentration (mol/m<sup>3</sup>) Arrow Surface: Velocity field



shearVel(5)=1.666667e-9 Time=0 s Surface: Concentration (mol/m<sup>3</sup>) Arrow Surface: Velocity field

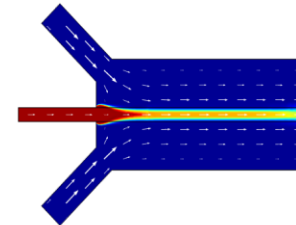


**Figure 13: Comsol models of flow focusing by adjusting flow rates. First image is pinched flow with 25  $\mu\text{l/m}$  flow rate, second at 50  $\mu\text{l/m}$ , third at 75  $\mu\text{l/m}$ , and the last at 100  $\mu\text{l/m}$**



13 shows this using the finite element analysis software package COMSOL to simulate flow of different species with various flow rates. Since we use vacuum-driven flow, direct control of fluid flow at the inlets is not possible. Instead, the inlet sizes had to be adjusted to control the flow into the device.

### **3.3.2 FABRICATION**

The process of etching a channel into a glass wafer requires microfabrication. We used a combination of photolithography with wet etching. Microfabrication can become very complicated and time consuming as mentioned for the existing DLD and roll over sorting method; however, in order to achieve a roll-over device, depth needs to be added to the device which required the use of wet etching. Unlike DLDs and roll-over devices, our device is fabricated with relatively large millimeter-sized features. The micron level features that effect particle sorting will come from the mesh.

To fabricate these glass channels, a mask of the channel was designed using AutoCAD. The glass wafers used come coated with chromium and photoresist from the manufacturer (TELIC, Valencia, CA). To remove the first layer of photoresist we place our mask over the wafer and expose it using UV light. Once exposed, the photoresist can be developed and removed using sodium hydroxide. Once the photoresist is removed, a layer of chromium is be exposed. This is removed next by etching with chromium etchant. The exposed glass is then etched using hydrofluoric acid (HF). HF etches this

glass at a rate of 7 microns per minute. The desired channel depth of 70 microns requires 10 minutes to etch. Finally, the remaining photoresist and chromium are removed.

### **3.3.3 ASSEMBLY**

Once the glass has the desired etched channel, the access holes are drilled. The mesh is then placed into the channel. A sheet of laminate is then placed in the etched glass channel and the device is placed into the laminator. The laminator heats the laminate and creates a seal between the glass and the laminate.

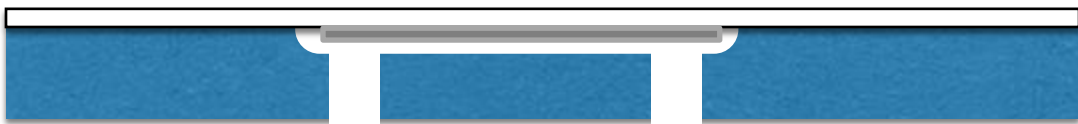


**Figure 14: Schematic of roll over device assembly**

### 3.4 SPECIFIC AIM III

#### 3.4.1 EXPERIMENTAL DESIGN

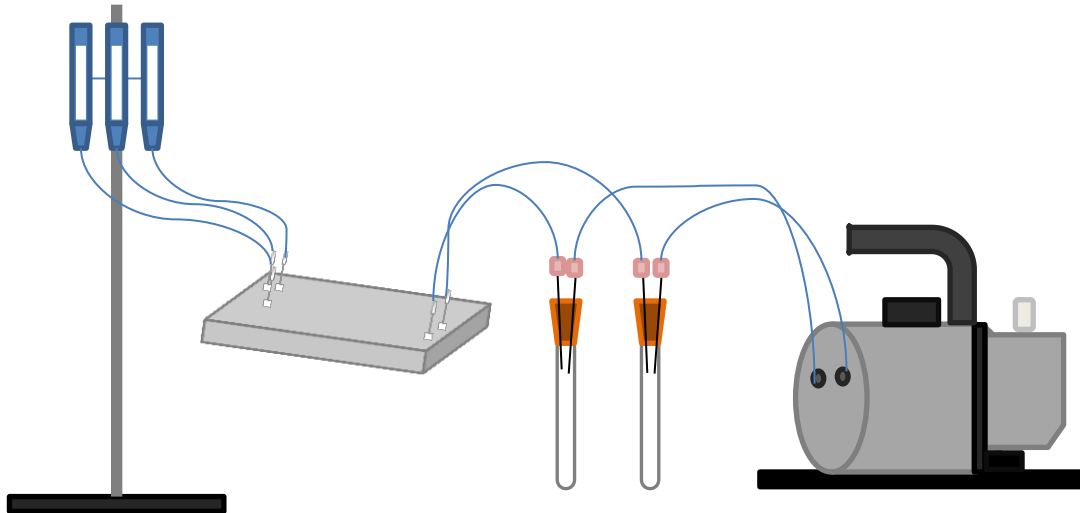


Figure 15: Schematic of experimental setup

The flow through and flow over devices were tested in two modes of flow. Experiments were conducted using both vacuum driven flow and head pressure. Displacement of particles through the device was determined by running fluorescent beads through the device. 5 micron diameter fluorescent beads were treated with bovine serum albumin (BSA) and introduced into the device. The particles were imaged using the Leica MZFLIII stereoscope.

### **3.4.2 FLOW THROUGH RESULTS**

The flow through device with a 78  $\mu\text{m}$  pore size mesh was imaged using the rigid flow through chip. 5  $\mu\text{m}$  beads and 10  $\mu\text{m}$  beads were sent through the device using head pressure to drive the flow. With a two second exposure time, green streaks can be seen as the beads flow through the device. Even though beads were treaded with BSA to prevent sticking, beads can be seen immobilized in the mesh.

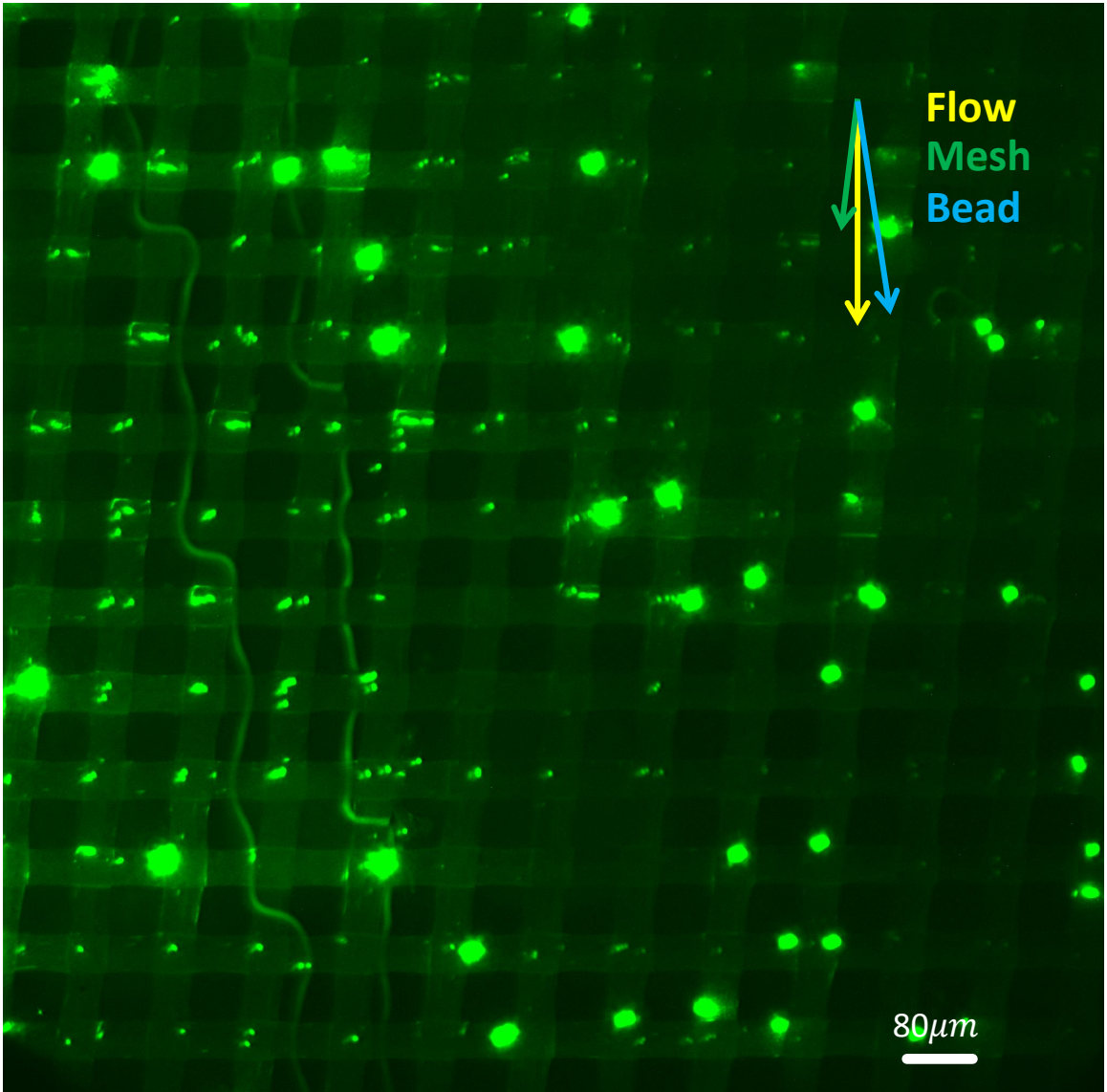


FIGURE 16: Head pressure driven flow of 5 and 10  $\mu\text{m}$  beads through a 78  $\mu\text{m}$  mesh

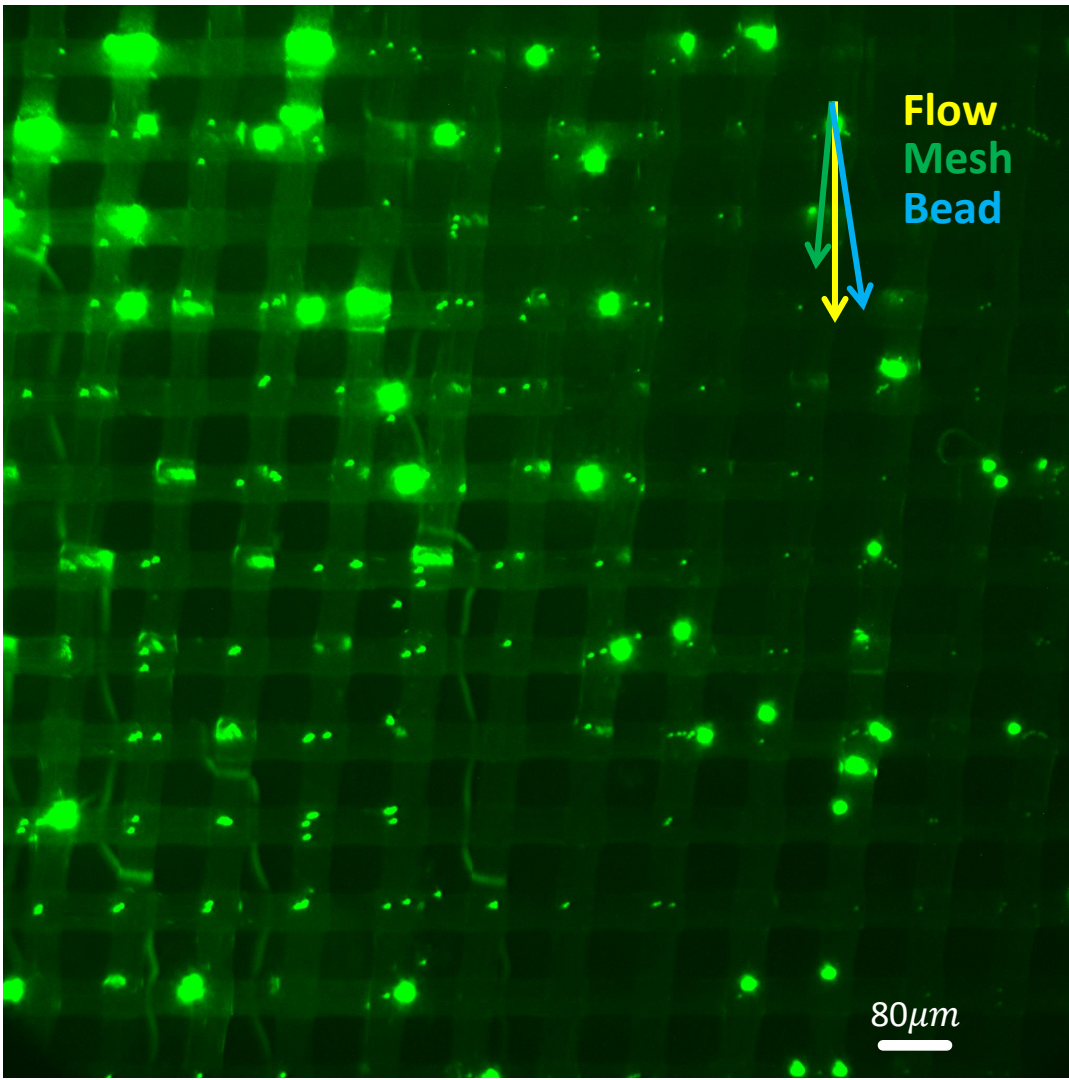
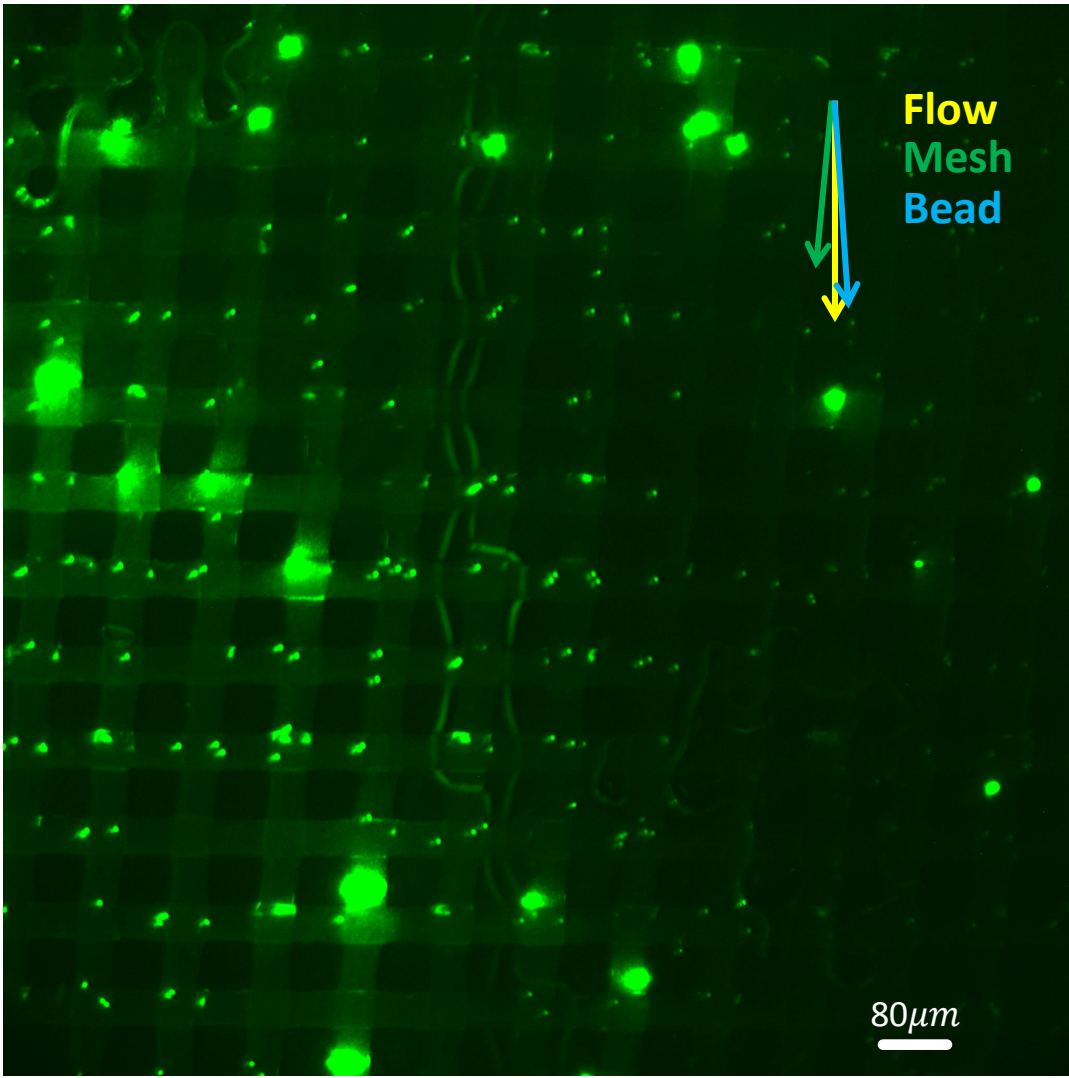


FIGURE 17: Head pressure driven flow of 5 and 10  $\mu\text{m}$  beads through a 78  $\mu\text{m}$  mesh



**FIGURE 18: Head pressure driven flow of 5 and 10  $\mu\text{m}$  beads through a 78  $\mu\text{m}$  mesh**

Figures 16-18 show the consistency at which the particles move through the mesh. This consistent movement is very similar to the movement of particles in a conventional DLD chip. A bead can be seen flowing relatively straight until it reaches the over/under junction of the mesh which for our model acts like a pillar would in a DLD. Once it reaches the junction, the particle stays in its original lamina and moves around the junction. If we treat the mesh as a normal DLD, the critical particle diameter would be 47

$\mu\text{m}$ . This means particles smaller than that should exhibit zigzag mode. This is exactly what we see from these 5  $\mu\text{m}$  particles. They are not displaced because they are smaller than the critical diameter. Image 3 shows the importance of separate flow lamina in the device. Two particles flowing through the same segment do not move around a junction until their respective lamina reach a junction, at which the bead will move around the junction.



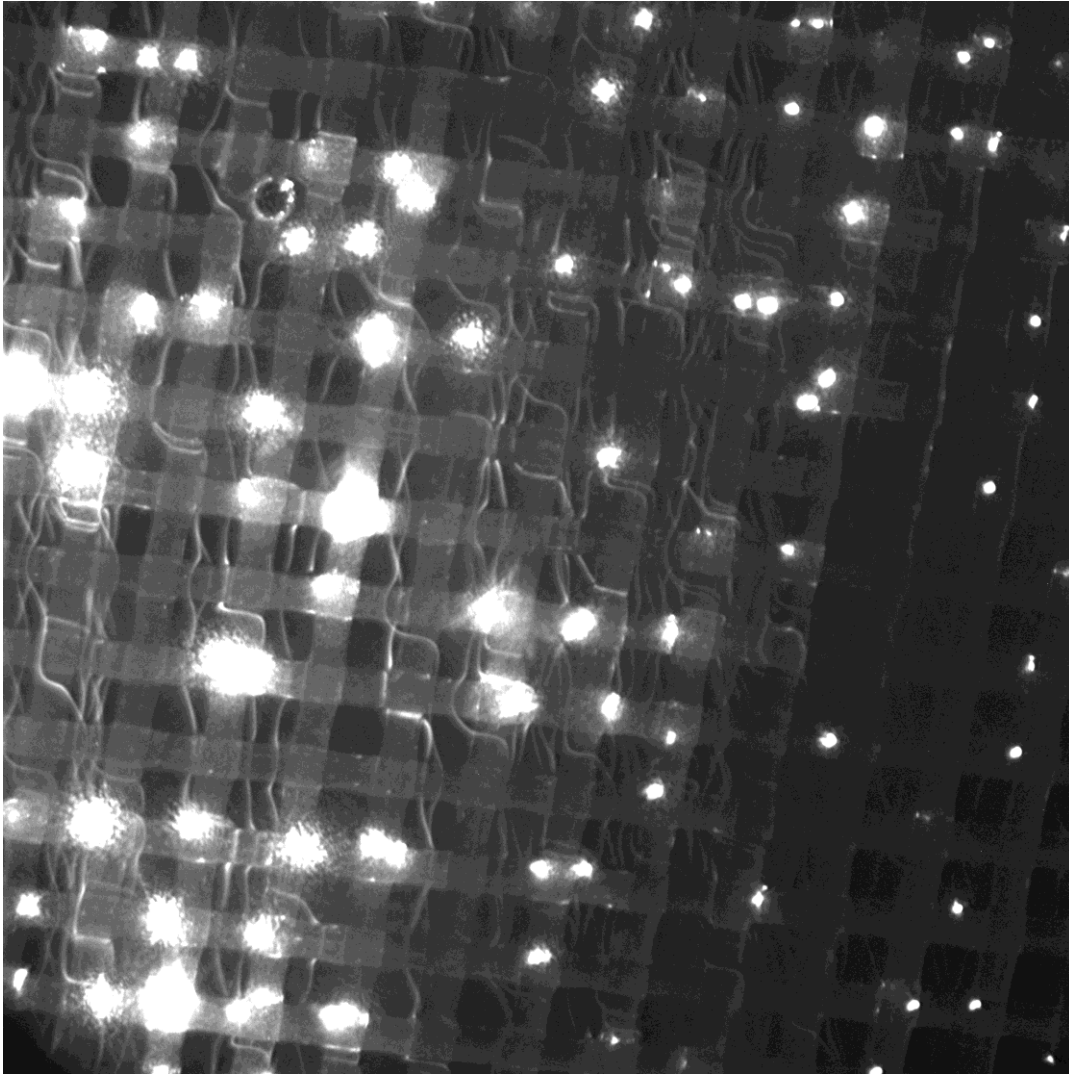


**FIGURE 19: Vacuum driven flow of 5  $\mu\text{m}$  beads through a 78  $\mu\text{m}$  mesh**

The previous figures show the flow through the device with head pressure driven flow. 5  $\mu\text{m}$  and 10  $\mu\text{m}$  beads can be seen interacting with the mesh in a very consistent manner. To determine the effects of higher flow rates on the interaction of the mesh with beads, the flow was increased using vacuum driven flow. For this experiment only 5  $\mu\text{m}$  beads can be seen flowing through the device. At higher flow rates, we noticed the beads

reacted with the mesh in an identical manner to which the head pressure driven beads reacted.

### **3.4.3 FLOW OVER RESULTS**

A 27  $\mu\text{m}$  pore size mesh was sealed into the channel of a flow over device and tested using head pressure driven flow. The particle size interacting with the mesh were 5  $\mu\text{m}$  beads. The device was imaged using the same equipment, a Lieca MZFLIII stereoscope. Beads were also treated with BSA to prevent them from settling into the mesh and becoming immobilized.

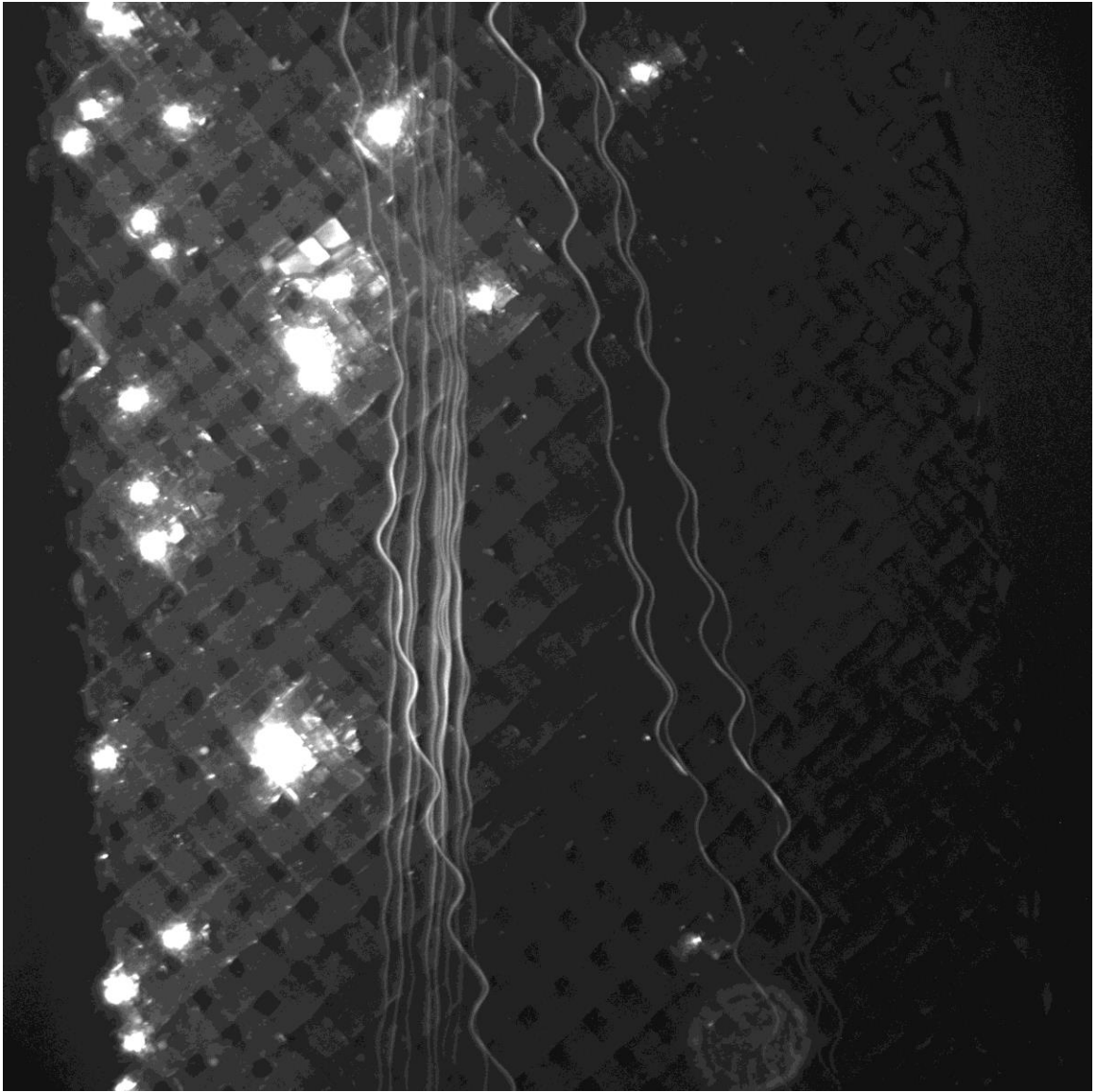


**FIGURE 20: Head pressure driven flow of 5  $\mu\text{m}$  beads over a 27  $\mu\text{m}$  mesh**

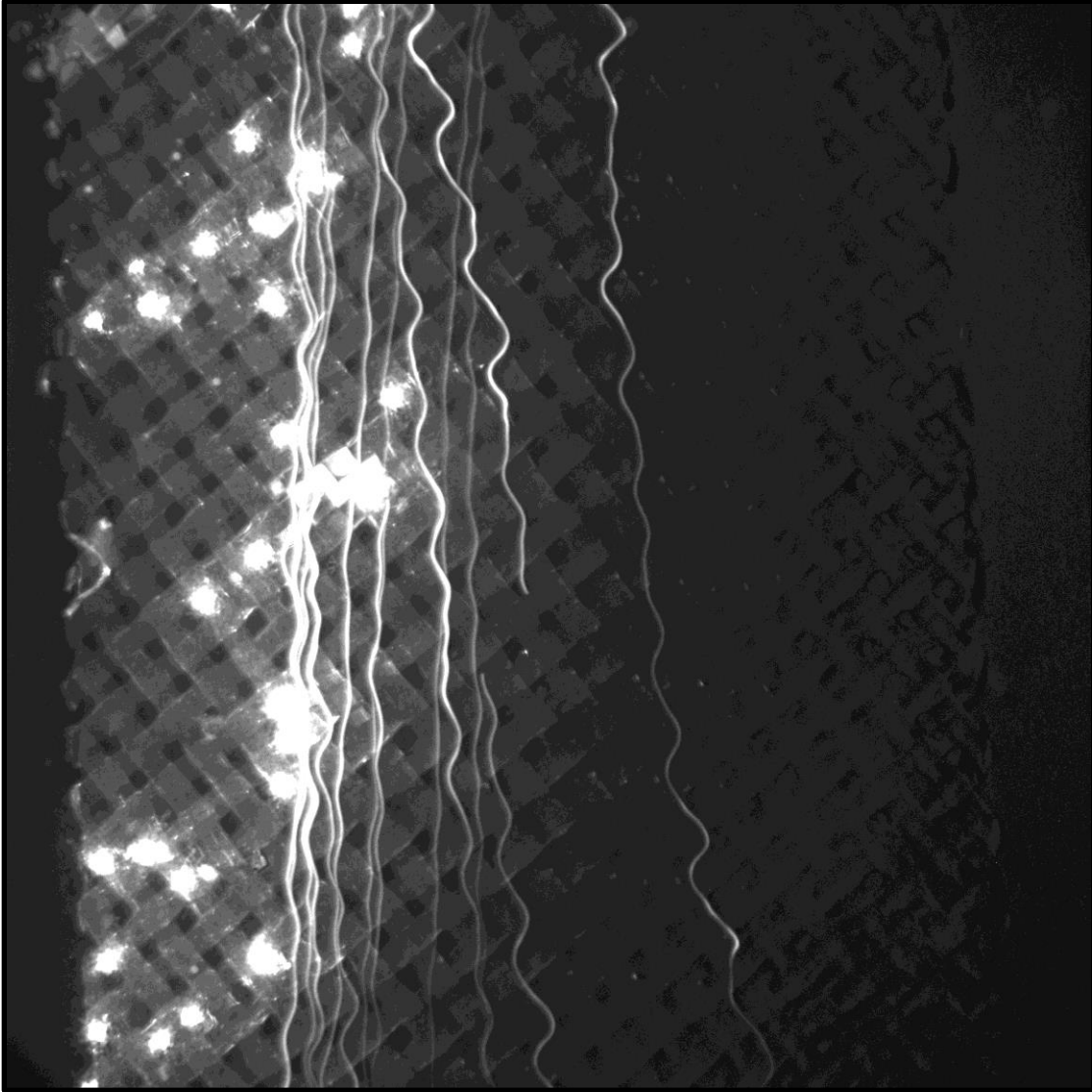


**FIGURE 21: Head pressure driven flow of 5  $\mu\text{m}$  beads over a 27  $\mu\text{m}$  mesh**

Figure 20 and 21 show the flow over device with the interaction of 5  $\mu\text{m}$  beads on a 27  $\mu\text{m}$  mesh. With head pressure driven flow, particle can be seen exhibiting two modes of flow. Particles will either flow over the device because they failed to settle to the bottom of the channel, or the particles will settle and as they roll across the mesh they will be displaced. Figure 20 and 21 show stream lines from beads that follow a straight path where are beads that settle are displaced to one side.

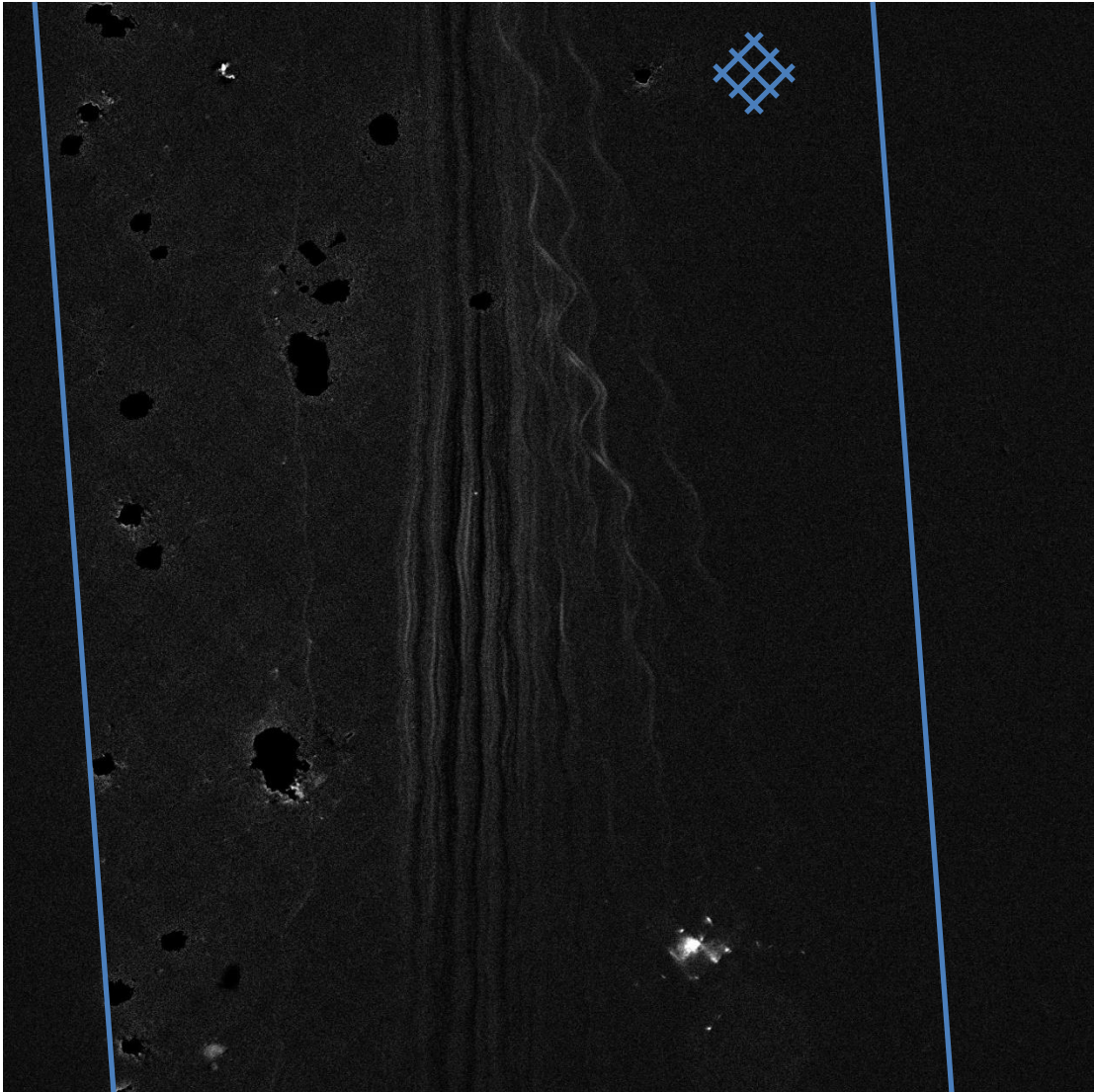


**FIGURE 22: Vacuum driven flow of 5  $\mu\text{m}$  beads over a 27  $\mu\text{m}$  mesh**

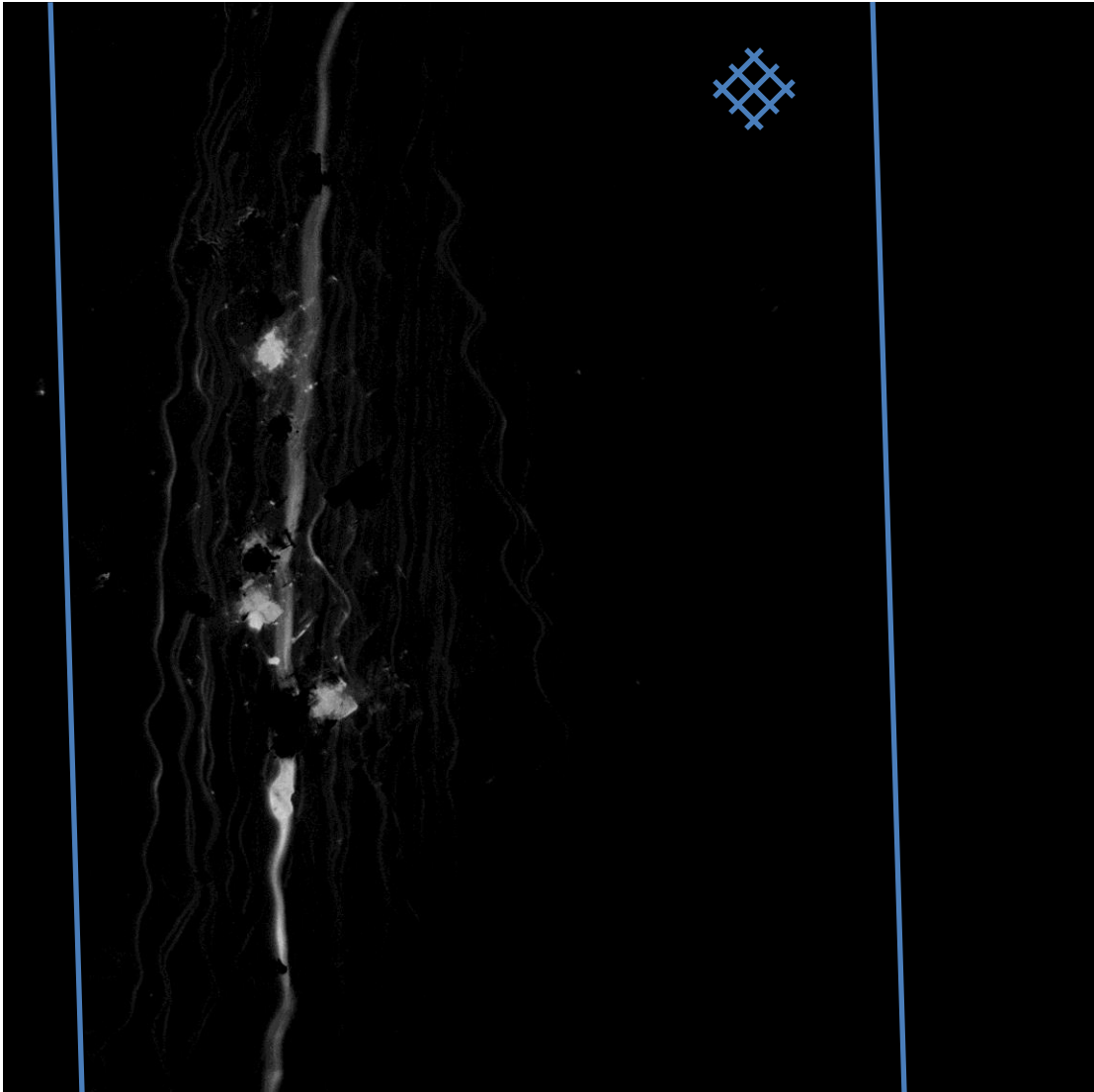


**FIGURE 23: Vacuum driven flow of 5  $\mu\text{m}$  beads over a 27  $\mu\text{m}$  mesh**

Figures 22 and 23 show the effects higher flow rates on particle movements in a roll over device. With vacuum driven flow, we notice the beads behave in a very similar manner to head pressure driven flow. Particles that do not interact with the mesh resulting in straight flow lines were as the few particles that do settle along the bottom of the channel exhibit displacement.

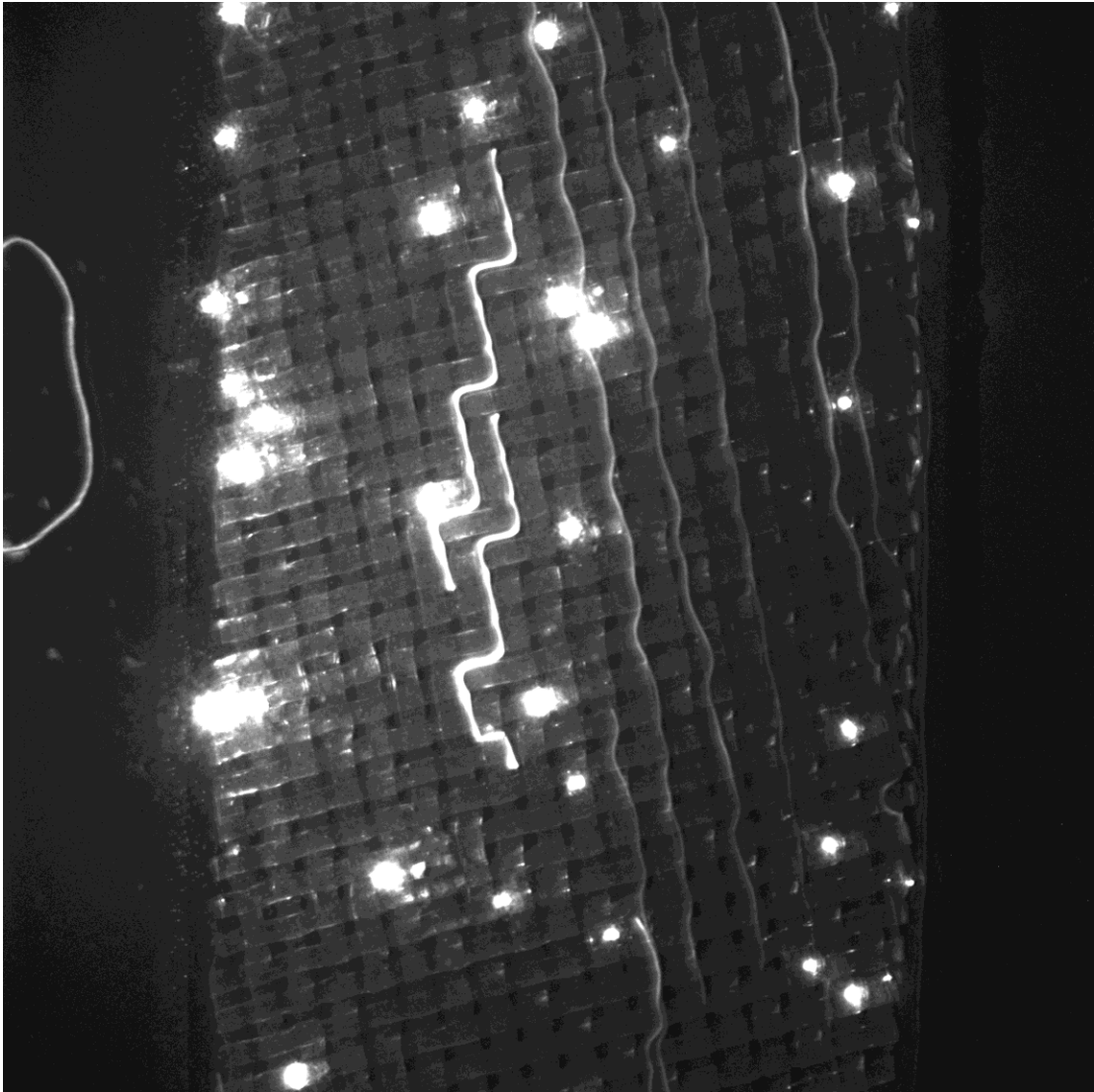


**FIGURE 24: Vacuum driven flow of 5  $\mu\text{m}$  beads over a 5  $\mu\text{m}$  twilled mesh**

Flow over a 5  $\mu\text{m}$  pore size twilled mesh resulted in very interesting results. Particles that settled experienced a very consistent and uniform displacement as the beads moved across the mesh. The “two over, one under” pattern of the mesh seemed to result in a consistent “3 down, 1 over” movement of the particle as it rolls through the mesh.

## **4. CONCLUSIONS**

### **4.1 FLOW-THROUGH DEVICES**

The results obtained from the flow through device were extremely encouraging. The movements of the beads flowing through the device look very similar to the movement exhibited in a classic DLD device. The difference between the DLD and our flow through device was the net lateral displacement of particles exhibiting zigzag mode. In a classic DLD device, particles smaller than the critical diameter will exhibit zigzag mode but have no net lateral displacement from where it originally began upstream. In the mesh based flow-through device, particles smaller than the critical diameter will exhibit zigzag mode; however, they will have a net lateral movement.

The parameters of the mesh based flow-through device need to be adjusted before it can separate particles of different sizes; however, the net lateral displacement of the particles smaller than the critical diameter give the flow-through device the ability to possibly sort particles from a fluid.

### **4.2 FLOW OVER DEVICES**

The flow over device exhibited very encouraging results as well. Particles that did settle into the mesh exhibited lateral displacement. By adjusting the channel height or flow



rates, more particles could be induced to settle resulting in more particles exhibiting the effects of the mesh as they flow across. 5  $\mu\text{m}$  particles flowing over the 27  $\mu\text{m}$  mesh exhibited displacement but not in the way the 5  $\mu\text{m}$  particles reacted to the 5  $\mu\text{m}$  twilled mesh. The twilled mesh resulted in very consistent and uniform displacement. Particles seemed trapped between the mesh resulting in a very effective roll over displacement. Moving forward, meshes of twilled patterning with smaller pore sizes could give optimal results for the flow over device.

### **4.3 FUTURE WORKS**

DLD devices have demonstrated their effectiveness as cell sorting devices; however, recent studies with CTC have demonstrated their ability to capture cells. DLD devices coated with anti-EpCAM have been used to capture cells. The mesh based flow-through device has the potential to be a great CTC capturing device if it were coated with anti-EpCAM. Due to its 3-dimensional geometry, the CTC's would interact with the mesh more, resulting in a higher chance of CTC capture.

## **5. REFERENCES**

1. A. A. S. Bhagat, H. Bow, H. W. Hou, S. J. Tan, J. Han and C. T. Lim, *Med. Biol. Eng. Compute.*, 2010,48,999-1014.
2. J. Autebert, B. Coudert, F.-C. Bidard, J.-Y. Pierga, S. Descroix, L. Malaquin and J.-L. Viovy, *Methods*, 2012, 57(3), 297-307
3. L. R. Huang, E. C. Cox, R. H. Austin and J. C. Sturm, *Science*, 2004, 304, 987-990.
4. E. L. Jackson and H. Lu, *Cur. Opin. Chem. Eng.*, 2013, 2, 389-404
5. Louthertback, Kevin. Microfluidic Devices for High Throughput Cell Sorting and Chemical Treatment. Vol. 73. No. 03. 2011.
6. Inglis DW, Davis JA, Austin RH, Sturm JC (2006) Critical particle size for fractioning by deterministic lateral displacement. *Lab Chip* 6:655-658
7. T. M. Sruires and S. R. Quake, *Rev. Mod. Phys*, 2005, 77, 977-1026
8. J. P. Beech, *Microfluidic separation and analysis of biological particles*, PhD, Lund University, 2011
9. J. A. Davis. Microfluidic Separation of Blood Components Through Deterministic Lateral Displacement, Doctor of Philosophy, Princeton University, 2008.
10. Norman KE, Moore KL, McEver RP, Ley K. *Blood*. 1995; 86:4417. [PubMed: 8541529]
11. Choi S, Park J-K. *Lab Chip*. 2007; 7:890. [PubMed: 17594009] Choi S, Park J-K. *Small*. 2009; 5:2205. [PubMed: 1963727]